

Interference of Dark Matter Solitons and Galactic Offsets

Angel Paredes¹ and Humberto Michinel

Facultade de Ciencias,
Universidade de Vigo, As Lagoas s/n,
Ourense, 32004 Spain

ABSTRACT

By performing numerical simulations, we discuss the collisional dynamics of stable solitary waves in the Schrodinger-Poisson equation. In the framework of a model in which part or all of dark matter is a Bose-Einstein condensate of ultralight axions, we show that these dynamics can naturally account for the relative displacement between dark and ordinary matter in a galactic cluster, whose recent observation is the first empirical evidence of dark matter interactions beyond gravity. We argue that future observations might bear out or falsify this coherent wave interpretation of dark matter offsets.

arXiv:1512.05121v1 [astro-ph.CO] 16 Dec 2015

¹e-mail:angel.paredes@uvigo.es

1 Introduction

The nature of dark matter is one of the most important open problems in fundamental physics. Projected experiments and astronomical observations are expected to shed new light on this question in the next decade [1].

In this context, the first evidence of dark matter (DM) non-gravitational self-interaction has been recently reported for the Abell 3827 cluster [2] ($z \approx 0.1$), where a displacement of the stars with respect to the maximum density of its DM halo has been observed, for some of the merging galaxies[3]. Possible explanations for this offset within the Λ CDM model comprise casual alignment with other massive structures that might influence the results from gravitational lensing, astrophysical effects affecting the baryonic matter, tidal forces or simply wrong identification of lensed images [4]. Even if these causes cannot be fully excluded, meticulous observations and simulations have shown that any such interpretation is unlikely to explain the collected data [4, 5]. This tension with collisionless dark matter models [5] suggests the necessity of considering other possibilities as, *e.g.* self-interacting dark matter, that yields a drag force slowing down the galactic DM distribution while leaving the standard model sector unaffected [3, 4, 5]. Nonetheless, requiring that the drag induces the offset implies a lower bound for the cross section that is in tension with upper bounds derived from other observations, as carefully discussed in [6]. Thus, the Abell 3827 cluster presents a challenging puzzle that opens up questions of crucial importance to understand the nature and dynamics of DM.

In this work, we address the problem of the measured offset using the scalar field dark matter (ψ DM) model [7, 8, 9], which considers a Bose-Einstein condensate (BEC) of non-relativistic ultra-light axions (ULAs) of mass m_a subject to Newtonian gravity and that was introduced to solve difficulties of Λ CDM (*e.g.* missing satellites problem and cusp-core problem[10]), while maintaining the successful phenomenology of the model at cosmological scales [11, 12]. Impressive numerical simulations [13] resolving largely different length scales have recently given support to this expectation. These extremely light scalar particles can arise in string theory constructions, *e.g.* [14] and other extensions of the standard model, *e.g.* [15]. Light scalars can also naturally appear as composites of hidden theories like the random UV field theory scenario [16].

We will show that the wave-like coherent nature of BECs severely affects the collisional dynamics of dark matter clumps, providing important effective forces even in the absence of explicit local interactions between the elementary dark matter constituents. We then discuss the possible relevance of this phenomenon to the puzzling observations described above.

2 Mathematical model

In the condensed scalar field scenario, the DM dynamics is governed by a Schrödinger-Poisson equation[17, 18, 19] for the mean-field wave-function ψ of the dark matter distribution:

$$i \hbar \partial_t \psi(t, \mathbf{x}) = -\frac{\hbar^2}{2m_a} \nabla^2 \psi(t, \mathbf{x}) - G m_a^2 \psi(t, \mathbf{x}) \int \frac{|\psi(t, \mathbf{x}')|^2}{|\mathbf{x}' - \mathbf{x}|} d^3 \mathbf{x}', \quad (1)$$

where $|\psi|^2$ is the particle number density, G the gravitational constant and t and \mathbf{x} are time and position. For simplicity, we disregard cosmological evolution of the scale factor and the contribution of baryonic matter to the gravitational field, implicitly assuming that they do not play a prominent role in the processes studied below. Although a local interaction term $\lambda |\psi|^2 \psi$ can be added to (1) [11, 20], we will restrict ourselves to the simplest $\lambda = 0$ case [7, 12, 13] that, as we show below,

is enough to describe the observed behaviour. Notice, however, that drag forces appear in similar mathematical models for optical systems with non-linear terms $\lambda \neq 0$, *e.g.* [21].

Equation (1) can be recast in terms of adimensional quantities:

$$\begin{aligned} i \partial_t \psi(t, \mathbf{x}) &= -\frac{1}{2} \nabla^2 \psi(t, \mathbf{x}) + \Phi(t, \mathbf{x}) \psi(t, \mathbf{x}), \\ \nabla^2 \Phi(t, \mathbf{x}) &= 4\pi |\psi(t, \mathbf{x})|^2. \end{aligned} \quad (2)$$

Following [22], the adimensional unit of length, time and mass correspond to:

$$\left(\frac{8\pi \hbar^2}{3m_a^2 H_0^2 \Omega_{m0}} \right)^{\frac{1}{4}} \approx 121 \left(\frac{10^{-23} \text{eV}}{m_a} \right)^{\frac{1}{2}} \text{ kpc}, \quad (3)$$

$$\left(\frac{3}{8\pi} H_0^2 \Omega_{m0} \right)^{-\frac{1}{2}} \approx 75.5 \text{ Gyr}, \quad (4)$$

$$\left(\frac{3}{8\pi} H_0^2 \Omega_{m0} \right)^{\frac{1}{4}} \frac{\hbar^{\frac{3}{2}}}{m_a^{\frac{3}{2}} G} \approx 7 \times 10^7 M_\odot \left(\frac{10^{-23} \text{eV}}{m_a} \right)^{\frac{3}{2}}. \quad (5)$$

We have taken $H_0 = 67.7 \text{ km}/(\text{s Mpc})$ for Hubble's constant and $\Omega_{m0} = 0.31$ for the matter fraction of energy today.

Equation (2) yields localized, radially symmetric, self-trapped robust solutions

$$\psi(t, \mathbf{x}) = \alpha e^{i\beta t} f(\sqrt{\alpha}|\mathbf{x}|), \quad \Phi(t, \mathbf{x}) = \alpha \varphi(\sqrt{\alpha}|\mathbf{x}|), \quad (6)$$

which we will loosely call solitons. α is an arbitrary scaling constant, the propagation constant is $\beta = 2.454\alpha$, the soliton mass is $M_{sol} = \int |\psi|^2 d^3\mathbf{x} = 3.883\sqrt{\alpha}$ and its diameter (full width at half maximum) is $d_{sol} = 1.380/\sqrt{\alpha}$. $f(\cdot)$ and $\varphi(\cdot)$ are functions that can be computed numerically. In terms of dimensionful quantities, the mass and size of the solitons are related by:

$$M_{sol} d_{sol} \approx \frac{5.36 \hbar^2}{m_a^2 G} \approx 4.6 \times 10^{10} \left(\frac{m_a c^2}{10^{-23} \text{eV}} \right)^{-2} \text{ kpc} M_\odot, \quad (7)$$

where M_\odot is the solar mass. In order to be reasonably self-contained, we give more details on these solutions and also discuss the numerical methods used for the computations in the appendix (section 7).

Finally, let us remark that these stationary states have been independently discussed in several physical contexts: foundations of quantum mechanics[19, 23], cold trapped atoms[24, 25], QCD-axions[26] and ultralight DM[27, 28]. This often overlooked formal coincidence indicates that studies concerning equation (1) can have deeply multidisciplinary implications.

3 Numerical simulations

In ψ DM, galactic dark matter distributions consist of a core which can be identified with a soliton surrounded by a background also governed by Eq. (2) and evolving in time and space with uncorrelated phases[13, 22, 29].

In this work, we propose that the offset of Abell 3827 [3] can come from the repulsion between coherent DM clumps (the solitonic cores) in phase opposition, without any extra local interactions. We show by numerical simulations that destructive interference can provide a large effective force

acting on the cores. This repulsion between robust wave lumps is well known in soliton systems, from nonlinear optics[30, 31] to atomic physics[32, 33, 34], where the mathematical description of the phenomena is similar to the theory of coherent DM waves.

In ref. [3], observations of DM concentrations with mass of the order of $10^{11}M_{\odot}$ surrounding stellar distributions separated by around 10 kpc were presented. Taking these values for M_{sol} and d_{sol} in equation (7), we find $m_a c^2 \approx 2 \times 10^{-24} \text{eV}$. We will fix this benchmark value for the simulations below. In section 5, we provide a discussion on previous observational constraints on m_a and on their relevance to the phenomenon described here.

First, we have analyzed the collision of two DM solitons by numerically integrating (2) with the initial condition:

$$\psi(t=0, \mathbf{x}) = \alpha f(\sqrt{\alpha}|\mathbf{x} - \mathbf{x}_0|)e^{i(v \cdot \mathbf{x})} + \alpha f(\sqrt{\alpha}|\mathbf{x} + \mathbf{x}_0|)e^{-i(v \cdot \mathbf{x} - \Delta\phi)} \quad (8)$$

where $2|\mathbf{x}_0|$ is the initial separation, $2v$ the initial relative velocity, $\Delta\phi$ the relative phase and α is related to normalization as described in section 2 (adimensional units). Previous studies of this sort with $\Delta\phi = 0$ can be found in [20, 35]. We use a split-step pseudo-spectral algorithm, known as beam propagation method [36, 37] (see the appendix for technical details). It is worth quoting other powerful numerical methods that have been recently developed for the Schrödinger equation with nonlocal terms[38, 39].

As expected, see *e.g.*[40] for a discussion in nonlinear optics with a particular nonlinear potential, the outcome largely depends on the relative phase and speed. In the case of phase opposition, destructive interference creates a void region between the solitons which can induce a bounce. For phase coincidence, the solitons merge into a single matter lump (which for large initial velocities eventually splits again). Interference fringes appear for large velocities [20, 35].

We must underline that in this work, for the first time to our knowledge, the effect of coherent DM waves on luminous matter has been calculated, by adding to our simulations test particles following classical trajectories in the gravitational field generated by the DM wave. These particles, initially located at the soliton centers, are a toy representation of the stars and can be shifted from the DM density peaks in a collision, as we show in figure 1. In figure 2, we plot the comparison between the trajectories of the point particle and the DM projected mass maximum. In order to check the limitations of this particle model, we have made use of the well known fact that Schrödinger equation can be cast into a hydrodynamic form through the Madelung transformation [41]. This allows us to develop a fluid toy model in which luminous matter is described as a spatially extended cloud (see the appendix for more details). As it can be seen in the inset of figure 2, both models display a good qualitative agreement.

Even if the collision in phase opposition is the simplest case, luminous vs. DM shifts can happen in more general situations. Figure 3 shows an example with four galaxies. Initial conditions are four solitons of mass $M_{sol} = 0.72M_{\odot}$ each, located at the vertices of a square of diagonal 40 kpc and initial velocities of 100 km/s towards the center, with phases 0, $\pi/2$, π and $3\pi/2$, respectively. When the solitons approach each other, their phase gradients induce a rotation of the DM cloud, with ordinary matter lagging behind. It is worth mentioning that stationary rotating solutions of Eq. (1) have been discussed in [42, 43].

Interference also plays an important role in asymmetric collisions if the phase difference between the lumps remains a well-defined quantity during the process. As an estimation, take $|\beta_1 - \beta_2|\Delta t_{col} \lesssim 1$ where β_1 and β_2 are the propagation constants of each soliton and Δt_{col} is the duration of the collision. In terms of the soliton mass:

$$\beta(\text{Myr}^{-1}) = 4.33 \left(\frac{M_{sol}}{10^{11}M_{\odot}} \right)^2 \left(\frac{m_a c^2}{10^{-23}\text{eV}} \right)^3. \quad (9)$$

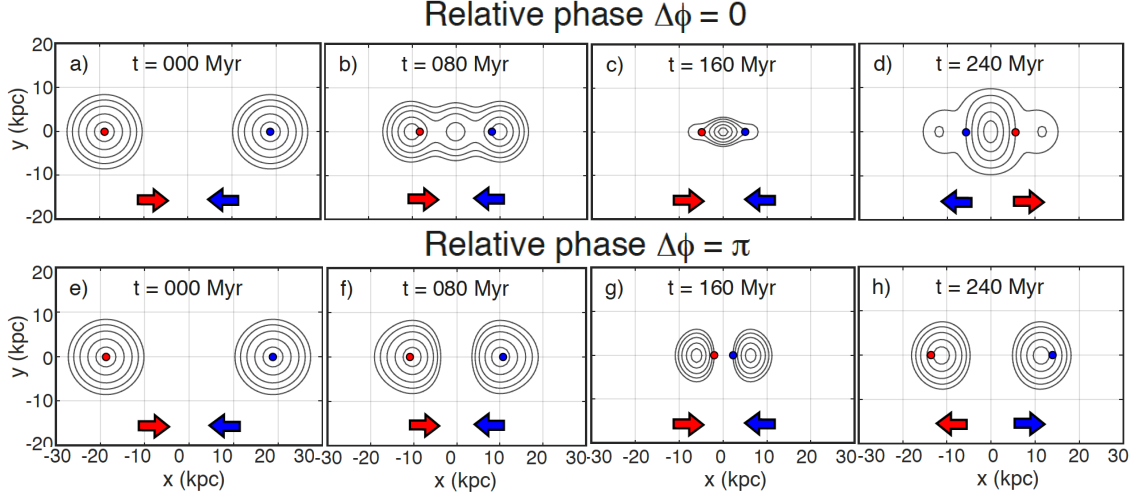


Figure 1: Simulation of the head-on collision of two DM solitons with $M_{sol} = 10^{11}M_{\odot}$, centers initially separated by 40 kpc and relative velocity 200 km/s. The contours show the projected DM mass density integrated over z . Dots are the point particles representing the center of gravity of ordinary matter in each lump and arrows indicate the direction of their velocity. Panels a)-d) show different instants of a simulation in which the solitons are launched in phase coincidence and merge. The sequence e)-h) corresponds to phase opposition and the DM clouds bounce back.

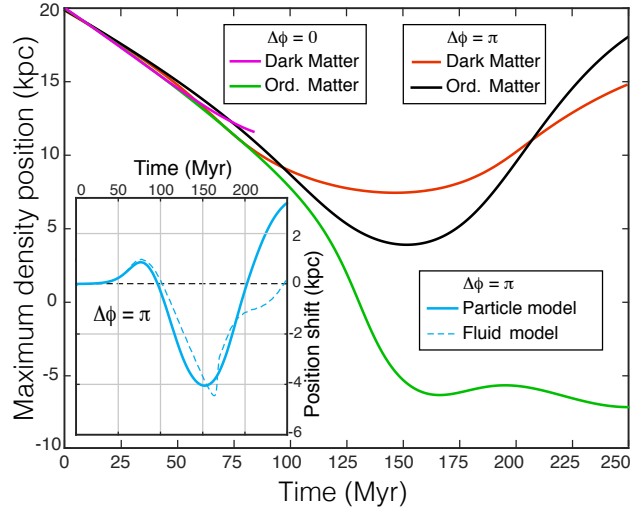


Figure 2: Time evolution of the position of the maximum density of DM and the test particle representing the stars for the simulations of figure 1. For the collision in phase opposition, corresponding to the second line of figure 1, offsets between the maxima of DM and ordinary matter are generated dynamically. The time evolution of the relative displacement is shown in the inset. In the case of phase coincidence ($\Delta\phi = 0$) no significant offset is observed. For $t > 85\text{Myr}$, the solitons have merged and the DM maximum lies at the center and thus, the pink line is cut at this point.

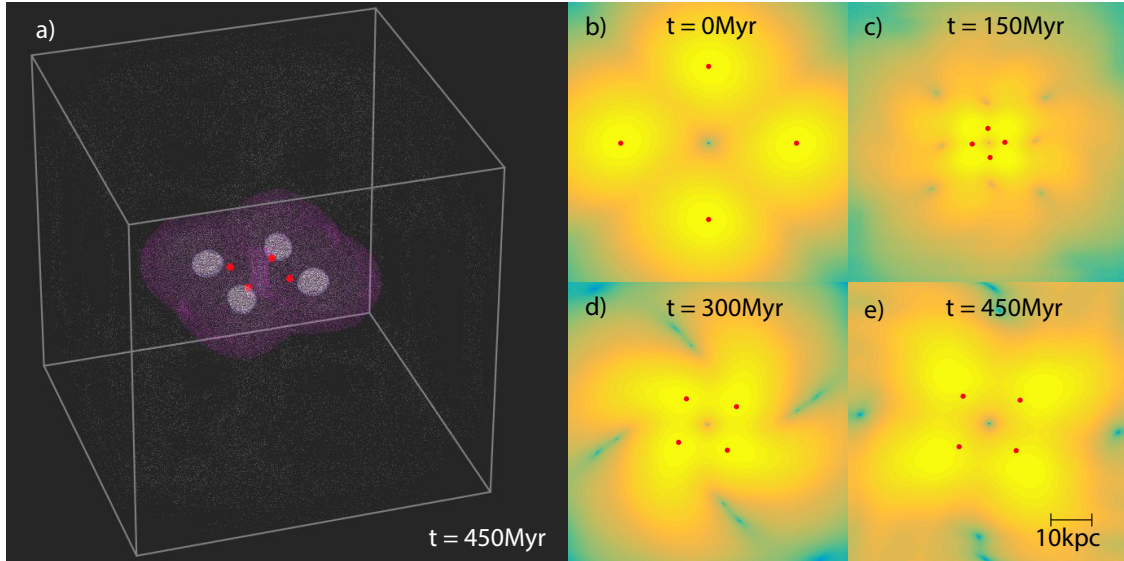


Figure 3: Simulation showing an example of ordinary matter vs. DM offset in a vortex-like configuration. In a), we show a three dimensional representation of the system at time $t = 450\text{Myr}$. The light and purple blobs are density iso-surfaces at 64% and 4% of the initial maximum density. Plots b)-e) are density color maps in logarithmic scale for the $z = 0$ plane at the times indicated in each picture. In all plots, the red dots are the point particles representing ordinary matter. The offset can be clearly appreciated at $t = 150\text{Myr}$ and $t = 450\text{Myr}$.

This yields:

$$\Delta t_{col}(\text{Myr}) \left(\frac{|M_{sol,1}|^2 - |M_{sol,2}|^2}{(10^{11} M_{\odot})^2} \right) \left(\frac{m_a c^2}{10^{-23} \text{eV}} \right)^3 \lesssim \frac{1}{4.33}. \quad (10)$$

In section 4, a collision involving four solitons will be considered. It is easy to check that the condition (10) holds in that case.

4 Comparison with observations

We now show that, starting with separate solitons, the wave dynamics of equation (1) can generate the gross features of the Abell 3827 cluster[3]: there are two DM blobs, one comprising galaxy N.1, for which dark matter and stars are separated; and the other one comprising galaxies N.2-N.4. In the present scenario, the natural interpretation is that N.1 is in phase opposition to N.2 whereas N.3 and N.4 are in phase. Figure 4 shows the result of a simulation. Initially, four separate solitons with masses 0.72, 0.95, 1.28 and 1.1 times $10^{11} M_{\odot}$ are considered. Solitons 1 and 3 are heading soliton 2 with relative velocities of 220 and 180 km/s. Soliton 4 has an initial velocity of 900 km/s in the transverse direction, in order to agree with the redshift measured in[3]. See the appendix for a full characterization of the initial condition. After evolution, we find offsets similar to those displayed in [3]. Matching these qualitative features as in figure 4 obviously requires an appropriate choice of initial conditions but we remark that no special fine tuning is needed.

Obviously, the real conditions are far more complicated. Apart from the coherent solitonic core, DM of field galaxies includes a non-coherent halo with an approximate Navarro-Frenk-White profile, see[22] for a detailed discussion. When the cluster is formed, most of its matter will be

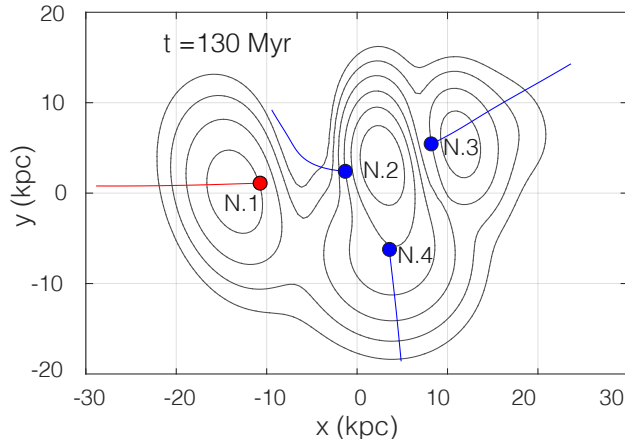


Figure 4: A numerical simulation generating an offset similar to the Abell 3827 cluster. The contour plot shows the projected mass density at a given time. Dots (numbered from N.1 to N.4) are the point particles representing the center of gravity of ordinary matter in each lump. Color lines indicate their trajectories from $t = 0$ to $t = 130\text{Myr}$. The qualitative agreement with observations reported in ref.[3], including the offset of N.1, is remarkable.

in an incoherent state with, at most, coherent lumps around the initial galactic cores (namely, around the stellar distributions). However, the presence of a large incoherent background does not necessarily change the qualitative features of the dynamics. Clearly, the effect of soliton-cluster halo interferences averages out to zero and can be neglected. Moreover, since the background density varies only mildly within the cluster, the gravitational forces it generates will not be dominant. A natural concern is whether incoherent matter might be attracted by the larger densities at the solitons, leading to smaller and more massive lumps. This is avoided if the kinetic energy of the incoherent wave is enough to impede its absorption, as in[22] for single galaxies. In fact, we have checked by numerical simulation that an incoherent background does not severely affect the process of figure 4.

5 Discussion on the axion mass

In this section, we briefly review the observational constraints on the axion mass m_a (see *e.g.* [29] and references therein) and their relation to our dark wave interpretation of the offsets. The essential hypothesis for our modeling is the existence of kiloparsec scale coherent cores. We remark that the dark matter density distributions for $R \lesssim 5 - 6\text{kpc}$ of galaxies like the Milky Way are subject to large uncertainties [44], [45] and therefore the assumption is neither confirmed nor excluded by direct inference of the galactic profiles.

It is natural to assume that we are in a scenario in which the cusp-core problem is solved by ψDM . By studying dwarf galaxies in this context, the authors of ref. [13] found a best fit of $m_a c^2 = (8.1_{-1.7}^{+1.6}) \times 10^{-23}\text{eV}$. By reanalyzing the same data, in ref. [29] it was shown that only a one-sided constraint $m_a c^2 < 1.1 \times 10^{-22}\text{eV}$ could be derived from those observations.

On the other hand, a lower bound $m_a c^2 > 10^{-24}\text{eV}$ comes from requiring that ψDM is indistinguishable from ΛCDM for the probes studied in[46]. This is a conservative lower bound, derived only from linear constraints on the cosmic microwave background. More stringent but also more

model dependent lower bounds were derived from nonlinear probes in [47, 48], see also [49] and [9] and references therein. Let us quote the result of [48], where it is found that data from the Hubble Ultra-Deep Field exclude axions with $m_a \lesssim 10^{-23} \text{eV}$ contributing more than half of DM.

The benchmark value of $m_a = 2 \times 10^{-24} \text{eV}$ that we have fixed in the simulations shown in the sections 3 and 4 comes from requiring solitonic cores with radius of the order of few kiloparsecs. We allow ourselves to use this value of m_a since it complies with the conservative lower bound of [46]. However, we envisage two possibilities in which these large cores could be present for larger values of m_a :

First, ULAs could be just a fraction of dark matter, relaxing to some extent the aforementioned stringent mass constraints, see *e.g.* [48]. Moreover, the total mass constituting each solitonic core would be smaller (for a fixed total dark matter mass), leading to larger radii by virtue of Eq. (7). The mechanism introduced in this paper can only cause a displacement of the ULA fraction of dark matter from the stars, but that can anyway render an offset for the DM center of mass.

Second, if a repulsive term $\lambda|\psi|^2\psi$, as first introduced in [11], is added to Eq. (1), the soliton radius would be larger than the one given in Eq. (7), see [25] for a detailed discussion.

If future observations and/or analysis indicate that ψ DM can only be realized with subkiloparsec cores for Milky Way-class galaxies, it would then be unlikely that soliton interactions play any role for providing relevant offsets within clusters like Abell 3827. Nevertheless, the analysis in this work would still play a role for the interaction between the solitonic cores. Understanding whether it might yield observational consequences is left for the future.

6 Conclusions

We have discussed the phenomenon of soliton interactions based on wave interference, which is relevant for any model of BEC dark matter relying on a Schrödinger-Poisson equation [7, 8, 9, 26, 50]. Large effective forces can be induced during collisions, in analogy with well known experiments in laboratory BECs and nonlinear optical systems.

If an ultralight scalar represents a significant fraction of DM, it is plausible that interference between dark waves can have observational consequences for galactic mergers and, in particular, it can explain the consequential results of [3]. The simplest setting for generating offsets is that of head on collisions in phase opposition (see figures 1 and 2), but we stress that they appear in more general situations (figures 3 and 4). The paramount hypothesis is the existence of coherent cores with radii of the order of few kiloparsecs. There are important qualitative differences with other models of DM: the force acting on DM is between the solitonic cores and not between a galaxy and the cluster halo. Moreover, the outcome depends on the value of the relative phase at the moment of the collision, which in a realistic situation could be taken as random. These two points can be tested if other similar mergers are observed with the level of detail achieved by [3] and can potentially reconcile the offset in [3] with the lack thereof in other systems [51, 52], which are in tension in models with particle-like interactions [6]. In the present work, we have considered an extremely simplified description of galactic dynamics which is enough to understand the gross features that can be expected from a wavelike behavior of DM. It would of course be desirable to incorporate these features in more detailed simulations as, for instance, those reported in [45] or [52].

Thus, we expect that through future theoretical progress and astrophysical observations, the scientific community will be able to discern the present scenario from models with explicit DM self-interactions or other logical possibilities. Finally, it is worth pointing out that, due to the formal coincidence of the governing equations, refined control of trapped atoms [24] and optical

media[53] introducing gravity-like interactions might allow for laboratory analogue simulators of galactic-scale phenomena.

7 Appendix: Technical details on numerical methods

In this appendix we describe a number of technical issues related to the numerical treatment of the Schrödinger-Poisson equation. We will use the form of the equation in terms of dimensionless quantities (2).

Stationary solution and initial conditions

Consider an ansatz with radial symmetry $\psi(t, \mathbf{x}) = e^{i\beta t} f(r)$, $\Phi(t, \mathbf{x}) = \varphi(r)$ where we have defined $r = |\mathbf{x}|$. Equation (2) is reduced to:

$$\begin{aligned} 0 &= -\frac{1}{2} \frac{d^2 f(r)}{dr^2} - \frac{1}{r} \frac{df(r)}{dr} + \varphi(r) f(r) + \beta f(r) \\ 0 &= \frac{d^2 \varphi(r)}{dr^2} + \frac{2}{r} \frac{d\varphi(r)}{dr} - 4\pi f(r)^2 \end{aligned} \quad (11)$$

Moreover, β can be reabsorbed as $\tilde{\varphi}(r) = \varphi(r) + \beta$. In order to find the soliton solution, we fix $f(r=0) = 1$ and perform a standard shooting method by varying $\tilde{\varphi}(r=0)$. Regularity at $r=0$ ensures that there are no more free parameters and $\tilde{\varphi}(r=0)$ is fixed by requiring that $f(r)$ vanishes as $r \rightarrow \infty$. Since $\lim_{r \rightarrow \infty} \varphi(r) = 0$, the value of β is read from the large r behavior of $\tilde{\varphi}(r)$. We find that $\beta = 2.454$, $M_{sol} = 4\pi \int_0^\infty r^2 f(r)^2 dr = 3.883$ and the full width at half maximum of the density is $\text{fwhm} \equiv d_{sol} = 1.380$. The solution is depicted in figure 5. Notice that $\varphi(r)$ has been rescaled in order to refer both functions to the same axis ($\varphi(r=0) \approx -4.76$).

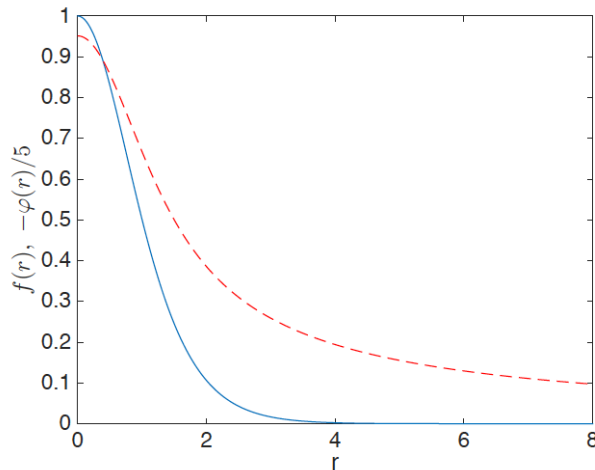


Figure 5: The functions $f(r)$ (solid blue) and $-\varphi(r)/5$ (dashed red) as defined in the text.

Due to the symmetry of equation (2), a whole family of solutions can be found by scaling. If we take $|\psi|(r=0) = \alpha$ for any $\alpha > 0$, then there is a solitary wave solution with $M_{sol} = 3.883\sqrt{\alpha}$, $\beta = 2.454\alpha$ and $\text{fwhm} = 1.380/\sqrt{\alpha}$.

Once a stationary solution is found and the functions $f(r)$, $\varphi(r)$ are explicitly known, Galilean invariance of the Schrödinger-Poisson equation allows us to write down the general boosted solution representing a soliton moving with constant velocity \mathbf{v} :

$$\begin{aligned}\psi(t, \mathbf{x}) &= \alpha f(\sqrt{\alpha}|\mathbf{x} - \mathbf{v}t|)e^{i(\alpha\beta t + \mathbf{v}\cdot\mathbf{x} - \frac{1}{2}|\mathbf{v}|^2 t)} \\ \Phi(t, \mathbf{x}) &= \alpha\varphi(\sqrt{\alpha}|\mathbf{x} - \mathbf{v}t|)\end{aligned}\quad (12)$$

This solution is used to define the initial conditions for the simulations, in which we consider initially separated solitons. For instance, the soliton collision of figure 1 has initial condition:

$$\psi(t=0, \mathbf{x}) = \alpha f(\sqrt{\alpha}\sqrt{(x+x_0)^2 + y^2 + z^2})e^{ivx} + \alpha f(\sqrt{\alpha}\sqrt{(x-x_0)^2 + y^2 + z^2})e^{-ivx+i\Delta\phi}\quad (13)$$

where $(-x_0, v)$, $(x_0, -v)$ are the (adimensional) initial position and velocity of each soliton, $\Delta\phi$ their relative phase and $3.883\sqrt{\alpha}$ the adimensional soliton mass. The test particles modeling the stars are initially placed at the center of the solitons with the same initial velocity. It is worth noticing that, due to Galilean invariance of equation (2), the same process can be thought of as, for instance, one soliton initially placed at $-2x_0$ moving with velocity $2v$ toward a static soliton with center at $x=0$. However, it is necessary to change the initial phase accordingly, namely:

$$\psi(t=0, \mathbf{x}) = \alpha f(\sqrt{\alpha}\sqrt{(x+2x_0)^2 + y^2 + z^2})e^{2ivx} + \alpha f(\sqrt{\alpha}\sqrt{x^2 + y^2 + z^2})e^{i(\Delta\phi - 2vx)}\quad (14)$$

Similarly, the initial condition used for the simulation leading to figure 4 is, explicitly:

$$\psi(t=0, \mathbf{x}) = \sum_{n=1}^4 \alpha_n f(\sqrt{\alpha_n}|\mathbf{x} - \mathbf{x}_n|)e^{i(\mathbf{v}_n\cdot\mathbf{x}_n + \phi_n)}\quad (15)$$

with $\alpha_1 = 544$, $\mathbf{x}_1 = (-0.175, 0.040, -0.060)$, $\mathbf{v}_1 = (67.4, -15.4, 69.2)$, $\phi_1 = 3.17$, $\alpha_2 = 947$, $\mathbf{x}_2 = (-0.027, 0.040, -0.060)$, $\mathbf{v}_2 = (5.04, -15.4, 69.2)$, $\phi_2 = 0$, $\alpha_3 = 1720$, $\mathbf{x}_3 = (-0.120, 0.040, -0.060)$, $\mathbf{v}_3 = (-46.0, -15.4, 69.2)$, $\phi_3 = 0.796$, $\alpha_4 = 1270$, $\mathbf{x}_4 = (-0.002, -0.108, 0.161)$, $\mathbf{v}_4 = (5.04, 41.3, -186)$, $\phi_4 = 0$. The plot displayed in figure 4 was rotated in the x-y plane for a better visualization.

Dynamical evolution

In order to compute temporal evolution in (2), we have used a split-step Fourier method, widely used in the integration of the nonlinear Schrödinger equation because of its stability and precision, see for instance references [36] and [37]. Schematically $\psi(t+dt, \mathbf{x}) = F^{-1}[e^{-i\mathbf{k}^2 dt/2} F[e^{i\Phi dt} \psi(t, \mathbf{x})]]$ where F is the three-dimensional Fourier transform. The preservation of the norm $\int |\psi|^2 d^3\mathbf{x}$ is automatic. At each step, we need to compute $\Phi(t, \mathbf{x})$ from Poisson equation. We do so using a finite difference scheme in a $N_x \times N_y \times N_z$ spatial grid. The discrete Poisson equation can be written as a linear problem $A \cdot B = C$ where A is the corresponding heptadiagonal $N_x N_y N_z \times N_x N_y N_z$ sparse matrix, B is a $N_x N_y N_z \times 1$ matrix with the value of the function Φ at each point of the grid and C includes the source and the boundary terms. This algebraic problem can be efficiently solved by an iterative symmlq method. We introduce boundary conditions as if all the mass were concentrated at the center of the computational grid (we compute in a reference frame in which the center of mass coincides with the center of the grid and the total momentum vanishes). The error introduced by these boundary conditions becomes negligible as the size of the computational box becomes much larger than the size of the region of interest. As an additional cross-check, we have also used a second method for solving Poisson equation, namely that of directly using Fourier transformation to deal with the laplacian. That implies periodic boundary conditions for Φ , which

also approach the physical boundary conditions as the box is made larger. In order to compute the classical trajectories for the point particles representing the standard model matter, we use Heun’s algorithm (a second order Runge-Kutta scheme), making use of the gravitational potential computed at each time step.

In order to test the precision of the algorithm, we first track the solution corresponding to a soliton moving with constant velocity, see figure 6, where the evolution of the modulus of the wave function at the center of the soliton is plotted. Numerical errors introduce two types of oscillations around the theoretical constant value. The short period oscillation is due to the velocity whereas a fluctuation with a longer period appears also for $\mathbf{v} = 0$. In any case, the figure shows that the method is stable and that fluctuations can be kept small.

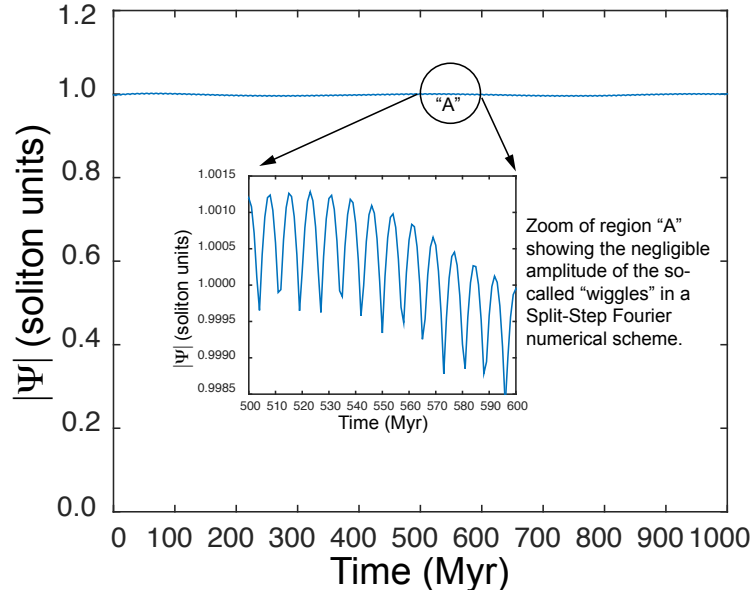


Figure 6: Simulation showing that the effect of spurious ”wiggles” due to the initial velocity of the galaxies is negligible in a split-step Fourier numerical scheme.

In order to further check the accuracy and validity of the computational methods, we have performed a series of auxiliary numerical simulations. In particular, we have calculated the effect on the dark matter soliton motion of different numerical schemes for integrating Eq. (2). Results for the example corresponding to figure 1 ($\Delta\phi = \pi$) are shown in fig. 7, where we plot the evolution of the DM soliton clouds, that of the stars and the corresponding offset. The maximum density position of the dark matter distribution is found by quadratic interpolation around the maximum value in the discrete grid. As it can be seen in the pictures, the differences between the methods are negligible for the evolution times that we have used in the paper.

A fluid toy model for ordinary matter

In this paper, we have used the simplest possible toy model for the ordinary matter, considering just test particles. More realistic descriptions would take into account that luminous matter is not point-like and that it sources the gravitational potential. However, these effects should not affect the qualitative conclusions presented in this work, since the offsets are generated by the interference force acting on the dark matter solitonic cores while not affecting the ordinary matter. As a first test

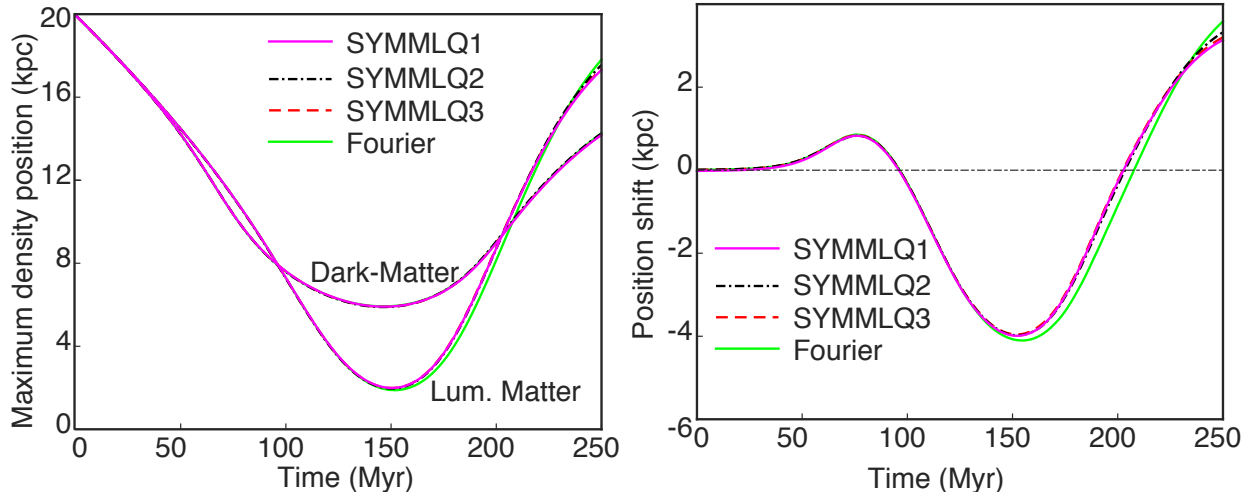


Figure 7: Left: comparison of the trajectories of the centers of dark-matter solitons and point-like galaxies obtained with four different numerical methods for Eq. (2). Symmlq1, symmlq2 and symmlq3 use a finite difference scheme to integrate Poisson equation at each step, with different spatial and temporal grids. For the Fourier line, a Fourier transform is used to solve Poisson equation. Right: Comparison of the offset calculated with the four different numerical methods

of this assertion, we have repeated the simulation for the collision in phase opposition (figs. 1 and 2) by considering the, arguably, simplest fluid model for ordinary matter: each galaxy is modeled by an independent Schrödinger equation coupled to Eq. (2). Thus, $i \partial_t g_i = -\frac{1}{2\gamma} \nabla^2 g_i + \gamma \Phi g_i$, where g_i correspond to the luminous matter distribution of each galaxy and γ is a parameter controlling its size ($\gamma = 2$ was taken for the figure). It is well known that nonlinear Schrödinger equations can be recast as fluid equations using a Madelung transformation (see, *e.g.* ref. [41]). Results are displayed in figure 8.

Acknowledgements

We thank D. Olivieri, J. Redondo and J. R. Salgueiro for useful comments. This work is supported by grants FIS2014-58117-P and FIS2014-61984-EXP from Ministerio de Ciencia e Innovación. The work of A.P. is also supported by the Ramón y Cajal program and grant EM2013/002 from Xunta de Galicia.

References

- [1] D. Bauer, J. Buckley, M. Cahill-Rowley, R. Cotta, A. Drlica-Wagner, J. L. Feng, S. Funk, J. Hewett, D. Hooper, A. Ismail, M. Kaplinghat, A. Kusenko, K. Matchev, D. McKinsey, T. Rizzo, W. Shepherd, T. M. Tait, A. M. Wijangco, and M. Wood, “Dark matter in the coming decade: Complementary paths to discovery and beyond,” *Physics of the Dark Universe*, vol. 7-8, pp. 16 – 23, 2015.

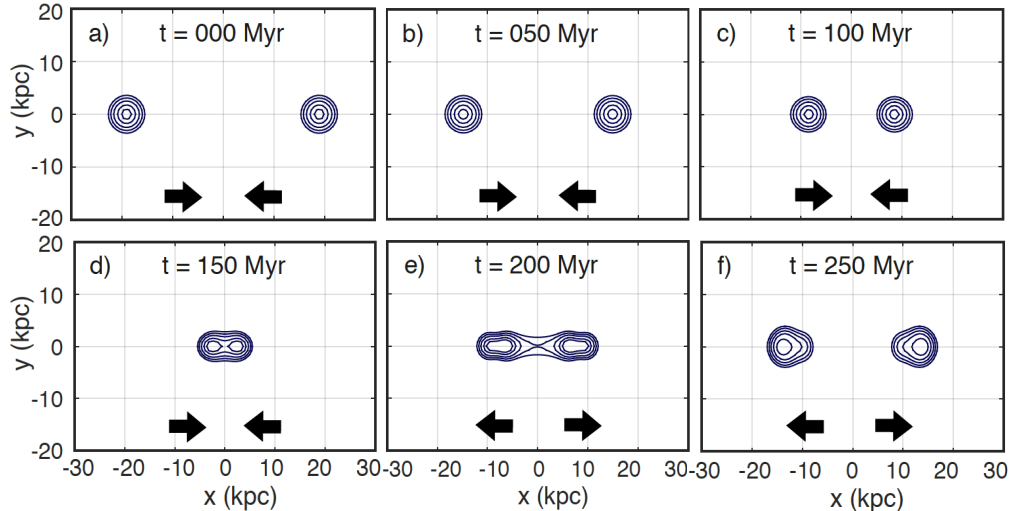


Figure 8: Simulation of the evolution of a widespread distribution of luminous matter, showing a qualitative behavior similar to the point particle model. For the simulation, we used a system of two mutually incoherent nonlinear Schrödinger equations, coupled to the system of Eq (2) given in the paper. The trajectory of the center of gravity of the luminous matter has been tracked and compared with the evolution of the "point galaxies" in the inset of fig. 2, with good qualitative agreement.

- [2] E. R. Carrasco, P. L. Gomez, T. Verdugo, H. Lee, R. Diaz, M. Bergmann, J. E. H. Turner, B. W. Miller, and M. West, "Strong gravitational lensing by the super-massive cd galaxy in Abell 3827," *The Astrophysical Journal Letters*, vol. 715, no. 2, p. L160, 2010.
- [3] R. Massey, L. Williams, R. Smit, M. Swinbank, T. D. Kitching, D. Harvey, M. Jauzac, H. Israel, D. Clowe, A. Edge, M. Hilton, E. Jullo, A. Leonard, J. Liesenborgs, J. Merten, I. Mohammed, D. Nagai, J. Richard, A. Robertson, P. Saha, R. Santana, J. Stott, and E. Tittley, "The behaviour of dark matter associated with four bright cluster galaxies in the 10 kpc core of Abell 3827," *Monthly Notices of the Royal Astronomical Society*, vol. 449, no. 4, pp. 3393–3406, 2015.
- [4] L. L. R. Williams and P. Saha, "Light/mass offsets in the lensing cluster Abell 3827: evidence for collisional dark matter?," *Monthly Notices of the Royal Astronomical Society*, vol. 415, no. 1, pp. 448–460, 2011.
- [5] M. Schaller, A. Robertson, R. Massey, R. G. Bower, and V. R. Eke, "The offsets between galaxies and their dark matter in cold dark matter," *Monthly Notices of the Royal Astronomical Society: Letters*, vol. 453, no. 1, pp. L58–L62, 2015.
- [6] F. Kahlhoefer, K. Schmidt-Hoberg, J. Kummer, and S. Sarkar, "On the interpretation of dark matter self-interactions in Abell 3827," *Monthly Notices of the Royal Astronomical Society: Letters*, vol. 452, no. 1, pp. L54–L58, 2015.
- [7] S.-J. Sin, "Late-time phase transition and the galactic halo as a Bose liquid," *Phys. Rev. D*, vol. 50, pp. 3650–3654, Sep 1994.

- [8] A. Suárez, V. H. Robles, and T. Matos, “A review on the scalar field/Bose-Einstein condensate dark matter model,” in *Accelerated Cosmic Expansion* (C. Moreno González, J. E. Madriz Aguilar, and L. M. Reyes Barrera, eds.), vol. 38 of *Astrophysics and Space Science Proceedings*, pp. 107–142, Springer International Publishing, 2014.
- [9] D. J. E. Marsh, “Axion cosmology,” arXiv:1510.07633, 2015.
- [10] W. J. G. de Blok, “The core-cusp problem,” *Advances in Astronomy*, p. 789293, 2010.
- [11] J. Goodman, “Repulsive dark matter,” *New Astronomy*, vol. 5, no. 2, pp. 103 – 107, 2000.
- [12] W. Hu, R. Barkana, and A. Gruzinov, “Fuzzy cold dark matter: The wave properties of ultralight particles,” *Phys. Rev. Lett.*, vol. 85, pp. 1158–1161, Aug 2000.
- [13] H.-Y. Schive, T. Chiueh, and T. Broadhurst, “Cosmic structure as the quantum interference of a coherent dark wave,” *Nat Phys*, vol. 10, pp. 496–499, 07 2014.
- [14] A. Arvanitaki, S. Dimopoulos, S. Dubovsky, N. Kaloper, and J. March-Russell, “String Axiverse,” *Phys. Rev.*, vol. D81, p. 123530, 2010.
- [15] J. E. Kim and D. J. E. Marsh, “An ultralight pseudoscalar boson,” arXiv:1510.01701, 2015.
- [16] E. Kiritsis, “Gravity and axions from a random UV QFT,” *EPJ Web Conf.*, vol. 71, p. 00068, 2014.
- [17] M. Y. Khlopov, B. A. Malomed, and Y. B. Zeldovich, “Gravitational instability of scalar fields and formation of primordial black holes,” *Monthly Notices of the Royal Astronomical Society*, vol. 215, no. 4, pp. 575–589, 1985.
- [18] E. Seidel and W.-M. Suen, “Dynamical evolution of boson stars: Perturbing the ground state,” *Phys. Rev. D*, vol. 42, pp. 384–403, Jul 1990.
- [19] I. M. Moroz, R. Penrose, and P. Tod, “Spherically-symmetric solutions of the Schrödinger-Newton equations,” *Classical and Quantum Gravity*, vol. 15, no. 9, p. 2733, 1998.
- [20] A. Bernal and F. S. Guzmán, “Scalar field dark matter: Head-on interaction between two structures,” *Phys. Rev. D*, vol. 74, p. 103002, Nov 2006.
- [21] D. Feijoo, I. Ordóñez, A. Paredes, and H. Michinel, “Drag force in bimodal cubic-quintic nonlinear Schrödinger equation,” *Phys. Rev. E*, vol. 90, p. 033204, Sep 2014.
- [22] H.-Y. Schive, M.-H. Liao, T.-P. Woo, S.-K. Wong, T. Chiueh, T. Broadhurst, and W.-Y. P. Hwang, “Understanding the core-halo relation of quantum wave dark matter from 3d simulations,” *Phys. Rev. Lett.*, vol. 113, p. 261302, Dec 2014.
- [23] R. Harrison, I. Moroz, and K. P. Tod, “A numerical study of the Schrödinger-Newton equations,” *Nonlinearity*, vol. 16, no. 1, p. 101, 2003.
- [24] D. O’Dell, S. Giovanazzi, G. Kurizki, and V. M. Akulin, “Bose-Einstein condensates with $1/r$ interatomic attraction: Electromagnetically induced “gravity”,” *Phys. Rev. Lett.*, vol. 84, pp. 5687–5690, Jun 2000.

- [25] I. Papadopoulos, P. Wagner, G. Wunner, and J. Main, “Bose-Einstein condensates with attractive $1/r$ interaction: The case of self-trapping,” *Phys. Rev. A*, vol. 76, p. 053604, Nov 2007.
- [26] A. H. Guth, M. P. Hertzberg, and C. Prescod-Weinstein, “Do Dark Matter Axions Form a Condensate with Long-Range Correlation?,” *Phys. Rev.*, vol. D92, no. 10, p. 103513, 2015.
- [27] F. S. Guzmán and L. A. Ureña-López, “Gravitational Cooling of Self-gravitating Bose Condensates,” *Astrophys. J.*, vol. 645, pp. 814–819, July 2006.
- [28] P.-H. Chavanis and L. Delfini, “Mass-radius relation of newtonian self-gravitating Bose-Einstein condensates with short-range interactions. ii. numerical results,” *Phys. Rev. D*, vol. 84, p. 043532, Aug 2011.
- [29] D. J. E. Marsh and A.-R. Pop, “Axion dark matter, solitons and the cusp-core problem,” *Monthly Notices of the Royal Astronomical Society*, vol. 451, no. 3, pp. 2479–2492, 2015.
- [30] F. M. Mitschke and L. F. Mollenauer, “Experimental observation of interaction forces between solitons in optical fibers,” *Opt. Lett.*, vol. 12, pp. 355–357, May 1987.
- [31] Y. S. Kivshar and B. A. Malomed, “Dynamics of solitons in nearly integrable systems,” *Rev. Mod. Phys.*, vol. 61, pp. 763–915, Oct 1989.
- [32] S. L. Cornish, S. T. Thompson, and C. E. Wieman, “Formation of bright matter-wave solitons during the collapse of attractive Bose-Einstein condensates,” *Phys. Rev. Lett.*, vol. 96, p. 170401, May 2006.
- [33] J. H. V. Nguyen, P. Dyke, D. Luo, B. A. Malomed, and R. G. Hulet, “Collisions of matter-wave solitons,” *Nat Phys*, vol. 10, pp. 918–922, 12 2014.
- [34] V. M. Pérez-García, H. Michinel, and H. Herrero, “Bose-Einstein solitons in highly asymmetric traps,” *Phys. Rev. A*, vol. 57, pp. 3837–3842, May 1998.
- [35] J. A. González and F. S. Guzmán, “Interference pattern in the collision of structures in the Bose-Einstein condensate dark matter model: Comparison with fluids,” *Phys. Rev. D*, vol. 83, p. 103513, May 2011.
- [36] G. Agrawal, *Nonlinear Fiber Optics*. Academic Press, Academic Press, 2013.
- [37] T. Poon and T. Kim, *Engineering Optics with Matlab*. World Scientific, 2006.
- [38] S. Jiang, L. Greengard, and W. Bao, “Fast and accurate evaluation of nonlocal Coulomb and dipole-dipole interactions via the nonuniform fft,” *SIAM Journal on Scientific Computing*, vol. 36, no. 5, pp. B777–B794, 2014.
- [39] R. K. Kumar, L. E. Young-S., D. Vudragovic, A. Balaz, P. Muruganandam, and S. Adhikari, “Fortran and c programs for the time-dependent dipolar Gross-Pitaevskii equation in an anisotropic trap,” *Computer Physics Communications*, vol. 195, pp. 117 – 128, 2015.
- [40] A. Paredes, D. Feijoo, and H. Michinel, “Coherent cavitation in the liquid of light,” *Phys. Rev. Lett.*, vol. 112, p. 173901, Apr 2014.

- [41] E. Spiegel, “Fluid dynamical form of the linear and nonlinear Schrödinger equations,” *Physica D: Nonlinear Phenomena*, vol. 1, no. 2, pp. 236 – 240, 1980.
- [42] T. Rindler-Daller and P. R. Shapiro, “Angular momentum and vortex formation in Bose-Einstein-condensed cold dark matter haloes,” *Monthly Notices of the Royal Astronomical Society*, vol. 422, no. 1, pp. 135–161, 2012.
- [43] F. Guzmán and F. Lora-Clavijo, “Rotation curves of ultralight bec dark matter halos with rotation,” *General Relativity and Gravitation*, vol. 47, no. 3, 2015.
- [44] M. Pato and F. Iocco, “The Dark Matter Profile of the Milky Way: a Non-parametric Reconstruction,” *Astrophys. J.*, vol. 803, no. 1, p. L3, 2015.
- [45] F. Calore, N. Bozorgnia, M. Lovell, G. Bertone, M. Schaller, C. S. Frenk, R. A. Crain, J. Schaye, T. Theuns, and J. W. Trayford, “Simulated Milky Way analogues: implications for dark matter indirect searches,” arXiv:1509.02164, 2015.
- [46] R. Hlozek, D. Grin, D. J. E. Marsh, and P. G. Ferreira, “A search for ultralight axions using precision cosmological data,” *Phys. Rev. D*, vol. 91, p. 103512, May 2015.
- [47] D. J. E. Marsh and J. Silk, “A model for halo formation with axion mixed dark matter,” *Monthly Notices of the Royal Astronomical Society*, vol. 437, no. 3, pp. 2652–2663, 2014.
- [48] B. Bozek, D. J. E. Marsh, J. Silk, and R. F. G. Wyse, “Galaxy uv-luminosity function and reionization constraints on axion dark matter,” *Monthly Notices of the Royal Astronomical Society*, vol. 450, no. 1, pp. 209–222, 2015.
- [49] L. Amendola and R. Barbieri, “Dark matter from an ultra-light pseudo-Goldstone-boson,” *Phys. Lett.*, vol. B642, pp. 192–196, 2006.
- [50] P. Sikivie and Q. Yang, “Bose-Einstein condensation of dark matter axions,” *Phys. Rev. Lett.*, vol. 103, p. 111301, Sep 2009.
- [51] M. Markevitch, A. H. Gonzalez, D. Clowe, A. Vikhlinin, W. Forman, C. Jones, S. Murray, and W. Tucker, “Direct constraints on the dark matter self-interaction cross section from the merging galaxy cluster 1e 0657-56,” *The Astrophysical Journal*, vol. 606, no. 2, p. 819, 2004.
- [52] D. Harvey, R. Massey, T. Kitching, A. Taylor, and E. Tittley, “The nongravitational interactions of dark matter in colliding galaxy clusters,” *Science*, vol. 347, no. 6229, pp. 1462–1465, 2015.
- [53] R. Bekenstein, R. Schley, M. Mutzafi, C. Rotschild, and M. Segev, “Optical simulations of gravitational effects in the Newton-Schrödinger system,” *Nat Phys*, vol. 11, pp. 872–878, 10 2015.